Fizika Nizkikh Temperatur, 2007, v. 33, Nos. 6/7, p. 661–667

Structural formation and thermal relaxation of quench-condensed Kr films: effect on EPR spectrum of trapped hydrogen atoms

Yu.A. Dmitriev

A.F. Ioffe Physico-Technical Institute, 26 Politekhnicheskaya Str., St. Petersburg 194021, Russia
E-mail: dmitriev.mares@pop.ioffe.rssi.ru

Received October 20, 2006

Hydrogen atoms were trapped in a quench condensed Kr matrix and investigated by EPR. Each hyperfine component is a superposition of broad and narrow line. The spectrum of narrow lines shows an axial anisotropy of the hyperfine structure constant. The extent of the anisotropy is found to depend on both the deposition temperature, T_{dep}, and the temperature of the solid sample, T_{sample}. As T_{dep} increases, the broad lines diminish while the anisotropy of the spectrum of narrow lines becomes less pronounced. The spectrum of narrow lines originate from H atoms in well defined environments and is attributed to a superposition of two spectra given by the atoms in substitutional fcc and hcp sites. The spectrum of broad lines is assumed to originate from the atoms trapped in highly disordered regions in the lattice. These regions are found to start relaxing at T_{sample} as low as 12 K.

PACS: **68.55.–a** Thin film structure and morphology;
68.55.Ln Defects and impurities: doping, implantation, distribution, concentration;
76.30.–v Electron paramagnetic resonance and relaxation;
61.72.Nn Stacking faults and other planar or extended defects.

Keywords: thin films, trapped atoms, atomic spectra.

1. Introduction

In the last decades a large amount of the experimental and theoretical work has been focused on the properties of small clusters of inert-gas elements and their solids with pores on the nanometer scale. A highly porous media (gels) were obtained in experiments when a jet of helium containing small amounts of impurity atoms and molecules was injected into superfluid helium [1]. Synchrotron x-ray diffraction studies [2] provide evidence that these materials are made of particles or small clusters surrounded by, possibly, layers of solidified helium.

Another considerable effort has been spent on a closely-related problem: obtaining and studying disordered solids of pure rare gases the thermodynamically stable phase of which shows a crystalline order. Strzhemechny and coworkers [3] undertook x-ray diffraction investigations into the structure and morphology of low-temperature quench-condensed binary alloys of hydrogen with argon and krypton in search of possible highly amorphized states in both systems. They concluded that the states formed in as-grown samples are in many respect analogs of helium-impurity media. Atoms and small molecules are often used as probes to study microstructure of inhomogeneities in quench-deposited rare gave solids. Methane molecules matrix-isolated in rare gas solids have been used as such a probe [4–7]. High-resolution neutron scattering spectra of quench-condensed nonequilibrium CH_4/Kr samples showed two rotational transitions for lowest levels [4]. The authors attributed one of them to $J = 0 \rightarrow 1$ transition of the almost free CH_4 quantum rotor on a fcc substitutional site of the Kr lattice, while the other was interpreted as $J = 0 \rightarrow 1$ transition at hcp matrix sites caused by the presence of stacking faults or hcp crystallites. They also stressed that the different width of the lines makes it probable that fcc and hcp sites do not exist within the same crystallite as a result of individual stacking faults but are more likely originating from fcc and hcp crystallites. Two dominant sites for guest molecules were observed in Ar, Kr, and Xe hosts in experiments where high-resolution infrared absorption spectra were recorded for the ν_4 vibrational mode of CH_4 trapped in these rare gas solids [5]. Having analyzed the fine structure of the spectra,

annealing studies and effects of deposition temperature, the authors came to the conclusion that one of these two sites was for CH_4 molecules trapped in the normal cubic-close-packed environment while the other site was for CH_4 trapped in hexagonal-close-packed pockets induced by stacking faults formed during deposition.

Neutron scattering experiments on vapor deposited CH_4/Ar films [6] revealed sharp transitions which originated from CH_4 molecules in well defined environments. They were attributed to molecules in an undisturbed fcc site, a fcc site neighboring a stacking fault, an hcp site in hcp crystallites, and an hcp site within a single stacking fault. CH_4/Ne samples prepared by matrix condensation showed addition diffraction peaks of hexagonal regions in addition to broadened diffraction lines of the equilibrium fcc cubic lattice. This also means that stacking faults, creating locally hexagonal environments, must be present at high concentration [7]. Based on neutron and x-ray diffraction data on vapor deposited pure Kr [8], the authors reported the basic sample structures to be fcc and in some cases also hcp, which originated from fcc due to stacking faults.

The structure of condensed pure Kr films was also investigated in x-ray diffraction experiments by Menges and Löhneysen [9]. They observed only peaks which could be attributed to the fcc structure and stressed that no hints were found for the existence of the hcp structure. Strzhemechny et al. [3] examined quench-deposited Kr/H_2 and Ar/H_2 mixtures by x-ray diffraction. For lower nominal hydrogen fractions ($c \leq 10\%$) they saw only reflections that could be attributed to the (111) line from a krypton-rich cubic lattice.

Pulsed NMR was used to study ortho-H_2 as a dilute impurity in solid Ne, Ar, Kr, and para-H_2 [10]. Having analyzed a temperature dependence of the intramolecular nuclear-spin relaxation of isolated o-H_2 molecules, the authors came to the conclusion that the introduction of an o-H_2 molecule into solid p-H_2 is not accompanied by large distortions and random static crystal fields, while the Ne and Ar results, on the other hand, indicate lack of symmetry for significant crystal fields at o-H_2 sites. The authors also point out that these fields may reflect distortions that accompany the introduction of an o-H_2 impurity into the rare gas solids, either substitutionally or otherwise. They also considered another possibility of o-H_2 molecules preferentially collecting around disordered sites and found indirect evidences in favor of this. The case of H_2/Kr is more complex, and the relevant results indicate more symmetric fields, perhaps nearly axial. The authors suggester an intramolecular relaxation model based on a mixture of sites with large crystal fields of no symmetry (70%) and axial symmetry (30%).

Thus, comparing the above results, there remain some questions concerning the structure of nonequilibrium rare gas solids and immediate surroundings of the impurity particles in these solids. The aim of this study is to obtain additional information in order to resolve the problem using the matrix isolation and EPR techniques. Solid Kr is the most suitable object because of both the high sublimation temperature favorable for sample growing into small single crystals and the absence of the nuclear magnetic moments resulting in the high resolution spectra.

2. Experimental

The discharge part of the setup as well as the microwave cavity and the gas filling and purification system remained unchanged [11]. The major distinction is that the bottom of the quartz finger which served as the low temperature substrate was cooled by liquid He vapor. The substrate temperature was controlled by changing the vapor flow. This temperature was measured by a thermocouple located on the outside surface of the finger. To monitor the vapor temperature, a carbon-resistance thermometer was mounted inside the finger.

3. Results and discussion

Figure 1,*a* shows one of the spectra of trapped H atoms we obtained in the present experiments. The substrate temperature during deposition, T_{dep}, was about 6.5 K; the commonly used gas flows were: 0.4 and 0.6 mmole/h through channels A and B, respectively. The H_2 concentration in the mixture with Kr passed through the discharge was 5%. The concentration of molecular hydrogen in the solid sample estimated from geometry of the depo-

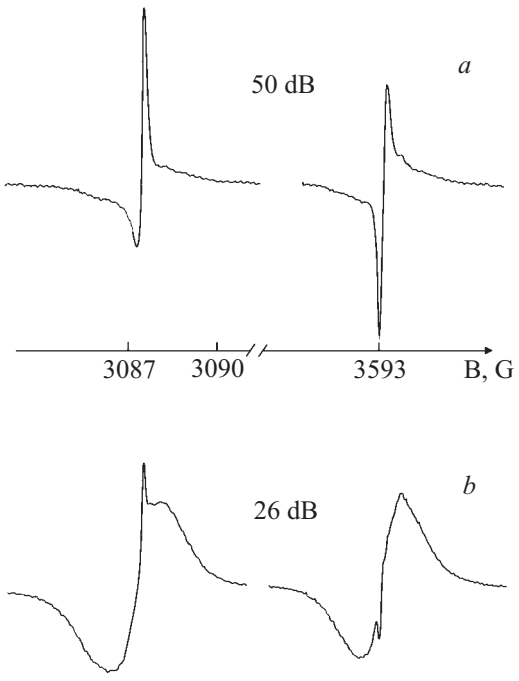

Fig. 1. The EPR spectrum of hydrogen atoms trapped in solid krypton at 6.5 K. The attenuation of the microwave power is 50 dB (*a*), 26 dB (*b*). The sample temperature during registration is 5 K. The microwave resonance frequency is 9410.82 MHz.

sition part of the set-up was $1.7 \cdot 10^{-4}$. The anisotropy of the lines clearly seen from Fig. 1,*a* and a superposition of narrow and broad lines which is obvious from Fig. 1,*b* is a characteristic feature of such spectra. We have found that the narrow lines saturate more readily than the broad ones. This behavior allows distinguishing any of these spectra.

We have also found that the spectrum of broad lines became less pronounced with increasing T_{dep}, while the extent of anisotropy and the linewidth of the spectrum of narrow lines decreased (Fig. 2,*a*). Figure 2,*b* shows a spectrum obtained after an annealing of short duration. Immediately after the annealing the sample temperature was decreased to 12 K and isotropic lines were recorded. Then the temperature was gradually increased to 23.5 K. Based on a comparison of the spectra taken in different runs, we came to the astonishing conclusion that the broad line position changed slightly from run to run. The only explanation is that the broad lines do not come from one type of centers, but from centers of several types. This assumption was verified by changing the sample temperature, T_{sample}. The broad line shape changed irreversibly as the sample temperature increased (Fig. 3). The

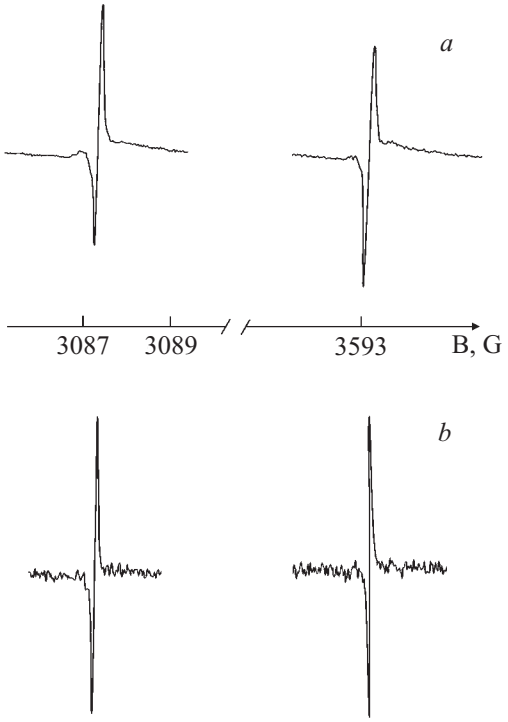

Fig. 2. EPR spectra of hydrogen atoms trapped in solid krypton at 10.5 K: *a* — before annealing; the sample temperature during recording is 11 K, the microwave resonance frequency is 9410.90 MHz, the attenuation of the microwave power is 50 dB; *b* — after annealing of short duration at approximately 40 K; the sample temperature during recording is 23.5 K, the attenuation of the microwave power is 40 dB, the spectrometer gain is increased.

Fig. 3. Effect of the sample temperature, T_{sample}, on the shape of the broad line. Only the low-field component is shown: *a* — after deposition on the substrate at 4.2 K, T_{sample} = 9 K; *b* — after a short annealing at 29 K, T_{sample} = 9 K; *c* — the sample temperature is gradually increased up to 25 K, T_{sample} = 25 K; *d* — the sample temperature is then decreased to 4.2 K, T_{sample} = 4.2 K.

lines not only appeared less intensive, but revealed a structure.

A detailed investigation of the transformations of the broad line shape showed that, as T_{sample} was increased in a gradual manner, the transformation finished in general before the temperature rose to about 20 K. Thus, we have observed a lattice relaxation at quite low temperatures when the Kr-atom self diffusion in the equilibrium lattice is insignilicant. During such a relaxation, some of the H atoms giving the broad lines were lost in the recombination process. Some transitions contributing to the broad line disappeared while other transitions appeared narrower becawse the surrounding became more regular. The narrow lines showed only a minor decrease in the intensity as the temperature increased to a moderate value. The broad EPR lines observed for a freshly prepared sample come from the H atoms trapped in the matrix in the highly disordered or even amorphous state. The former assumption seems to be more likely because it is generally agreed that no pure amorphous rare gas solids can be produced with experimentally attainable quenching rates [9]. On the other hand, the amorphous state might appear as a local structure not observed by x-ray or neutron diffraction methods. We suppose that the broad line spectrum is not associated with the porosity of the solid gas matrix. The reason for this assumption is that the number of pores starts to prevail at deposition temperatures below 35 K for

the Kr solid [12]. The pore concentration increases, the pore size distribution widens and its maximum shifts towards smaller sizes as the T_{dep} decreases in a rather gradual manner [12]. On the other hand, our results suggest a sharp increase of the intensity of the broad lines when T_{dep} is below 7 K. It is interesting that a diffuse intensity was observed in the neutron diffraction study of the quench condensed solid Kr [8]. The authors assumed that the diffuse intensity was due to continuously deformed unit cells. Thus, a local perturbation of the lattice relaxes over a large number of unit cells into unperturbed zones of the crystal. Our observation of the broad EPR lines supports the presence of such continuously distorted regions.

Another unusual result of the present study is the anisotropy of narrow lines. The spectrum parameters measured here, $A_{iso} = 1408.97(21)$ MHz and $g_{iso} = 2.00164(12)$, are close to the values reported earlier [13,14] for the substitutionally trapped H atoms. One can see from Fig. 1, that the axial anisotropy of the hyperfine structure constant A is well pronounced, while the g-factor anisotropy is not evident. We estimate the difference between perpendicular, $A_{\perp}$, and parallel, $A_{||}$, components to be about 3 MHz. This rather small anisotropy was possible to be observed because of the small linewidth which implies well defined surroundings of the trapped H atoms. The linewidth depends on both T_{dep} and T_{sample} and on the ranges from about 0.12 to 0.3 G. The axial anisotropy of the spectrum is a fingerprint of the axial crystal field at the H atom location. Let a and b be two amplitudes measured between the base line and the two peaks of the EPR line. Here a is the greater one. Then a/b ratio may be considered as a measure of the line anisotropy. In this way we found the anisotropy to decrease as the T_{sample} increased. This is evident from Fig. 4.

The extent of the anisotropy at a given T_{sample} depends on T_{dep}. For samples prepared at substrate temperatures below approximately 5 K and, especially, when the broad line spectrum was pronounced, the anisotropy to might persist up to temperatures of about 40–48 K (depending on the conditions during deposition). At these temperatures the solid gas layer started to evaporate in our experiments. Very recently, a characteristic desorption temperature of $T_{des} = 42$ K has been found for quench-condensed Kr films by means of high-frequency surface acoustic waves [15]. Thus, our estimation of T_{des} checks with the earlier observation. Even after a deep annealing of short duration, the spectrum might stay anisotropic, Fig. 4. As T_{sample} decreased, the line showed an increased anisotropy. The anisotropy may regain its initial extent. This depends in part on the maximum T_{sample} reached during annealing and on the annealing duration. The not fully reversible line shape suggests some structural relaxation or H atoms diffusion into other sites. On the other

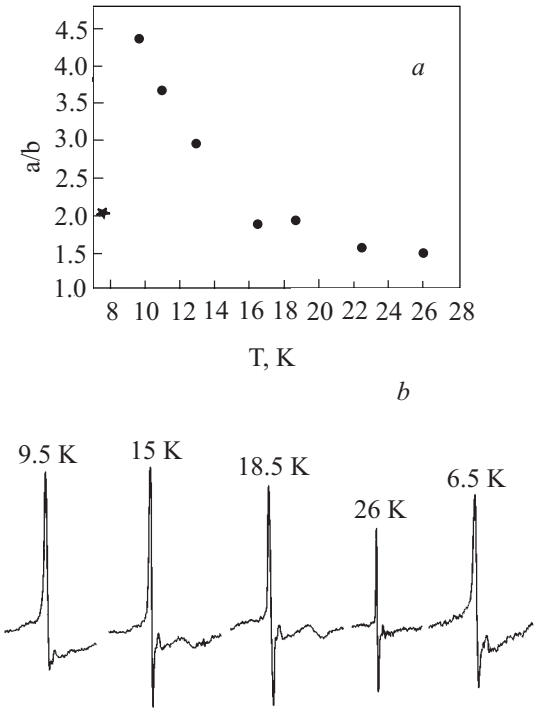

Fig. 4. The temperature dependence of the a/b ratio in one of the runs. The ratio serves as a tentative measure of the anisotropy (T_{dep} = 7 K, microwave power attenuation is 50 dB): *a* — T_{sample} is decreased (solid circles), T_{sample} is again lowered down (a star); *b* — tracing the low-field line through the temperature cycling; the last two lines are recorded at an amplification 1.5 times hidher.

hand, samples obtained at T_{dep} above approximately 10 K show spectra closer to the isotropic EPR spectrum, Fig. 2,*a*. After a short annealing, the spectrum intensity went down and the line shape changed to isotropic, Fig. 2,*b*. The transformation has occurred. This result is inherent in the spectra of samples obtained at high T_{dep}.

Figure 5 shows a reversible change in the line shape. The sample was prepared at T_{dep} of about 7 K and was subjected to intermediate annealing at 25 K, resulting in the broad lines going down. Being initially anisotropic, the lines grew isotropic at high temperatures and regained its initial shape after the sample was again cooled down to low temperatures. In the process, the amount of EPR centers dropped essentially, suggesting recombination of diffusing atoms. Interestingly, the shape variation had no effect on the line parameters, A_{iso} and g_{iso}. We suppose that the spectrum behavior described above may be explained assuming this spectrum to be a superposition of two spectra: one is due to H atoms trapped in fcc regions and the other, by atoms in hcp regions. Indeed, it was shown [16,17] that the hyperfine structure constant and the g-factor are governed mainly by the pair interaction between a trapped atom and host atoms and molecules. In this case, A and g are sensitive to the distance between the H atom and the host particles. These distances are the same

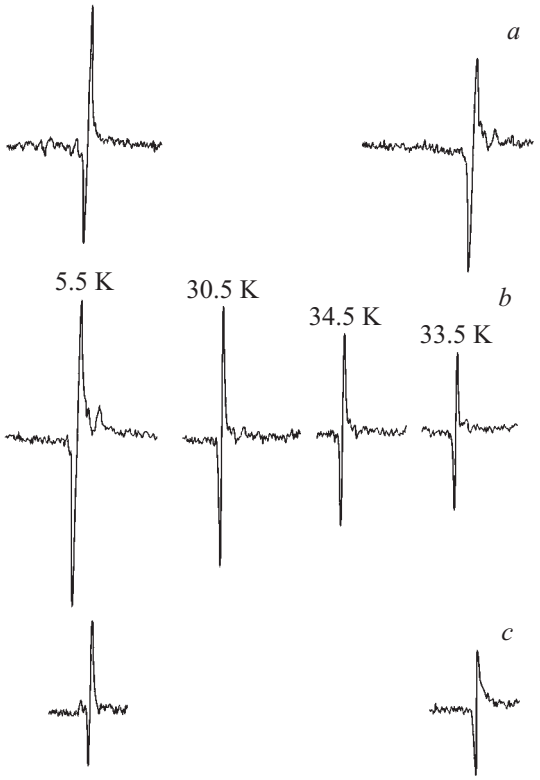

Fig. 5. The sample was prepared at T_{dep} of about 7 K and experienced intermediate annealing at T_{sample} = 25 K with the result of the broad lines going down: *a* — anisotropic EPR spectrum of H atoms in solid Kr, T_{sample} = 5.5 K; *b* — high-field component of the doublet showing a change with time of the isotropic line intensity; T_{sample} is indicated at the top; *c* — the spectrum regains its anisotropy after the sample temperature has been decreased again to T_{sample} = 5.5 K. The microwave power attenuation is 50 dB (*a*) and 40 dB (*b*, *c*).

for the immediate surroundings in fcc and hcp structures. The number of matrix atoms nearest to a trapped H atom is also equal for these two structures. So, the lines of the corresponding spectra are expected to coincide. The changes in the extent of the anisotropy are then explained by variations in the relative number of fcc (surroundings of cubic symmetry) and hcp (surroundings of axial symmetry) sites. In accordance with earlier observations [4–8] the hexagonal environment appears only under quench condensation conditions. The present results correlate well with the reported high stability of the hcp structure [6].

It was found in neutron experiments on CH_4 trapped in solid Ar [6] that the hcp crystallites, which were assumed to be the cause of the line at 0.59 meV, required 1 h annealing at T_{sample} = 80 K to disappear through recrystallization into fcc structure. That is why we have still observed, in some experiments, the EPR spectrum anisotropy even after a deep short annealing. On the other hand, the transformation at very low temperatures of a part of the hcp regions into fcc is evidenced by the irreversible anisotropy in Fig. 4. The irreversible decrease in the anisotropy upon a considerable change in T_{sample}, also observed in the present investigation, is most likely explained by the diffusion of H atoms occuring at a sufficiently high temperature with subsequent trapping. Since the major part of the lattice has the fcc structure, the extent of the spectrum anisotropy decreases again after trapping. In the present experiments, such a decrease is frequently accompanied by a decline in line intensity, which confirms the assumed diffusion. In turn, the reversible change in the anisotropy may be explained by: a) an effect which oscillations of the neighboring matrix atoms probably have on the anisotropy extent, b) an effect of fast motion of H atoms on the EPR line shape. With increasing temperature, the oscillations become more intensive resulting in a decreasing anisotropy. It was pointed [18] (molecular dynamics simulations of O_2 rotations in gas solids) that a small cage distortions around the impurity in the classical solids are diminished by lattice vibrations, which may lead to a nearly spherical cage geometry. Indeed, no anisotropy was reported for H atoms in the H_2 matrix despite the hcp equilibrium structure of solid hydrogen. Even in para-H_2 solid, where the EPR linewidth for trapped H atoms is about 0.1 G, the spectrum stays isotropic. Although as-prepared vapor deposited H_2 solids contain fcc regions which convert irreversibly to hcp upon annealing [19], it is commonly believed that the fcc structure constitutes only a minor part of the sample.

The isotropic spectra of H in H_2 may arise for two reasons: a smaller matrix shift of the hyperfine constant as compared with solid Kr; and large zero-point vibrations of the host molecules. The considerable change of the line shape at temperatures near 32 K (Fig. 5) was accompanied by a rapid decrease in the number of trapped H atoms. On the other hand, it has been mentioned above that for samples grown at T_{dep} closer to 4.2 K, the anisotropy may persist even at temperatures above 32 K. On those samples we observed a substantially slower decrease in line intensity at T_{sample} near 32 K. These results suggest that the rapid motion of diffusing H atoms averages the interaction with their surroundings and removes the EPR line anisotropy.

It is interesting to compare the present results with those obtained earlier [14]. In EPR studies of the thermal mobility of atomic hydrogen in solid Kr matrix, Vaskonen and co-authors observed no diffusion of substitutionally trapped H atoms up to the evaporation temperature of the matrix. Not indicated, this temperature is possibly above 30–40 K, for which we observed H-atom diffusion. The reason for this discrepancy is that the solids obtained in Ref. 14 cannot be considered as quench-condensed. Indeed, the deposition temperature was 22 K and not favorable for vacancy formation needed for the substitutional atoms to diffuse. The authors stressed that H atoms generated by UV-photolysis of HBr and HCl precursor molecules in solid Kr showed generally an octahedral trapping rather than a substitutional one. The H-atom

population in the octahedral sites of the as-deposited samples exceeded that in the substitutional sites by about two orders of magnitude [14]. Classen *et al*. [20] investigated acoustic properties of quench-condensed films of Ne and Ar and observed structural relaxation in a rather broad temperature region. For an Ar film condensed at 3.6, the relaxation was found [20] at temperatures in the range from 3.6 to 7.5 K and at 10, 12.7, and 13.9 K. These are well below T_{des} = 30 K for Ar [15]. The authors came to the conclusion that there is a rather broad spectrum of activation energies involved in the irreversible structural rearrangement. Hence, when the temperature is increased, more and more atomic rearrangements can take place, which requires overcoming higher energy barriers.

Using the double-paddle oscillator, White et al. [21] measured the shear modulus of thin films of Ar and Ne during annealing at cryogenic temperatures. For Ar and Ne films deposited at 1.2 and 1.3 K, respectively, they observed and studied a stiffening of the films at 10.407 and 20.155 K in Ar, and at 3.049 K in Ne. The desorption temperature for Ne is 8 K [15]. Obviously, one may expect a similar behavior of quench-condensed Kr films, i.e., structural relaxations at low temperatures in a broad temperature range. This is partly supported by the broad line transformation below 20 K observed in the present study. Hence, with a plenty of vacancies in the quench-condensed Kr, these structural rearrangements may sufficiently increase the atomic hydrogen diffusion to be recorded in our experiment. The EPR lines for H in Kr presented in Ref. 14 are isotropic. Based on the present findings, this result is expectable for a sample deposited at 22 K.

Prager and Langel [6] pointed out that a local hcp environment may be produced by stacking faults along the (111) direction of the fcc structure of the undisturbed matrix. One stacking fault creates two (111) planes with hcp surrounding and two planes of fcc symmetry facing the defect. An H-atom trapped in such a hcp surrounding would experience an axial crystal field. However, it takes several lattice constants for a distortion to relax. This would have effect on the hyperfine constant of the trapped atom and, possibly, broaden the line. Therefore, it seems more likely that the surrounding of the axial symmetry is associated with atoms trapped in hcp crystallites.

4. Conclusions

EPR spectra have been obtained for H atoms trapped in quench-condensed solid Kr. It was shown that the substrate temperature during deposition had a decisive effect on the shape of the hyperfine components. The experiments were conducted at T_{dep} ranging from 1.5 to 11 K. Mostly, each hyperfine component was a superposition of broad and narrow lines. At higher temperatures of the range, $T_{dep} \geq 10$ K, the broad lines were extremely weak or even unobservable. The intensity of these lines increased rapidly as the T_{dep} decreased from about 7 K. The broad lines were attributed to atoms trapped in a strongly disordered phase. As the temperature was raised, these lines revealed the structure suggesting a relaxation of this phase which happened at $T_{sample} < 20$ K. The narrow lines showed an axial anisotropy of the hyperfine structure constant. We presented experimental evidence suggesting that these lines are most likely caused by atoms trapped in hcp crystallites of the nonequilibrium solid Kr. The extent of the anisotropy decreased with increasing T_{dep}. The anisotropy was also found to depend on the sample temperature. In our experiments we obtained a rather large fraction of H atoms trapped in hcp crystallites, which are believed to be only a small fraction of the solid sample. One of possible reasons for this findings is attributed to the trapping process of H atoms and H_2 molecules. The incident hydrogen atoms and molecules lost only a small portion of their kinetic energy in collisions with the surface Kr atoms because of the large difference between the masses of the colliding particles. On the other hand this loss is much greater in H–H_2 and H_2–H_2 collisions. This may cause a nonuniform distribution of hydrogen over the solid sample and appearance of regions with sufficiently large hydrogen content. Since the energy difference between the hcp and fcc lattices is small, such hydrogen-rich regions being under nonequilibrium conditions might possibly bring about the hcp structure.

5. Acknowledgments

Thanks are due to M.E. Kaimakov for active participation in part of these investigations and for reading the manuscript.

1. E.B. Gordon, L.P. Mezhov-Deglin, and O.F. Pugachev, *JETP Lett*. **19**, 63 (1974).
2. V. Kiruykhin, B. Keimer, R.E. Boltnev, V.V. Khmelenko, and E.B. Gordon, *Phys. Rev. Lett*. **79**, 1174 (1997).
3. M.A. Strzhemechny, N.N. Galtsov, and A.I. Prokhvatilov, *Fiz. Nizk. Temp*. **29**, 699 (2003) [*Low Temp. Phys*. **29**, 522 (2003)].
4. M. Prager and W. Langel, *J. Chem. Phys*. **90**, 5889 (1989).
5. L.H. Jones, S.A. Ekberg, and B.I. Swanson, *J. Chem. Phys*. **85**, 3203 (1986).
6. M. Prager and W. Langel, *J. Chem. Phys*. **88**, 7995 (1988).
7. M. Prager, B. Asmussen, and C.J. Carlile, *J. Chem. Phys*. **100**, 247 (1994).
8. W. Langel, W. Schuller, E. Knözinger, H.-W. Fleger, and H.J. Lauter, *J. Chem. Phys*. **89**, 1741 (1988).
9. H. Menges and H. v. Löhneysen, *J. Low Temp. Phys*. **84**, 237 (1991).
10. M.S. Conradi, K. Luszczynski, and R.E. Norberg, *Phys. Rev*. **B20**, 2594 (1979).

11. R.A. Zhitnikov and Yu.A. Dmitriev, *Fiz. Nizk. Temp*. **24**, 923 (1998) [*Low Temp. Phys*. **24**, 693 (1998)].
12. S.A. Nepijko, I. Rabin, and W. Schulze, *Chem. Phys. Chem*. **6**, 235 (2005).
13. S.N. Foner, E.L. Cochran, V.A. Bowers, and C.K. Jen, *J. Chem. Phys*. **32**, 963 (1960).
14. K. Vaskonen, J. Eloranta, T. Kiljunen, and H. Kunttu, *J. Chem. Phys*. **110**, 2122 (1999).
15. M. Layer, A. Netsch, M. Heitz, J. Meier, and S. Hunklinger, *Phys. Rev*. **B73**, 184116 (2006).
16. F.J. Adrian, *J. Chem. Phys*. **32**, 972 (1960).
17. T. Kiljunen, J. Eloranta, and H. Kunttu, *J. Chem. Phys*. **110**, 11814 (1999).
18. Z. Li and V. A. Apkarian, *J. Chem. Phys*. **107**, 1544 (1997).
19. S. Tam and M.E. Fajardo, *Fiz. Nizk. Temp*. **26**, 889 (2000) [*Low Temp. Phys*. **26**, 653 (2000)].
20. J. Classen, J. Meier, M. Heitz, and S. Hunklinger, *Physica* **B263**–**264**, 163 (1999).
21. B.E White, Jr, J. Hessinger, and R.O. Pohl, *J. Low. Temp. Phys*. **111**, 233 (1998).